INTERNATIONAL JOURNAL OF HYDROGEN ENERGY 43 (2018) 9408–9412

Available online at www.sciencedirect.com

ScienceDirect

journal homepage: www.elsevier.com/locate/he

Energy loss of 100 keV hydrogen isotopes in materials for nuclear applications

M.G. Petaccia [a,*], J.L. Gervasoni [a,b]

[a] Comisión Nacional de Energía Atómica (CNEA), Centro Atómico Bariloche (CAB), Av. Exequiel Bustillo 9500, San Carlos de Bariloche, Río Negro, Argentina

[b] Consejo Nacional de Investigaciones Científicas y Técnicas (CONICET), Godoy Cruz 2290 (C1425FQB) Ciudad Autónoma de Buenos Aires, Argentina

ARTICLE INFO

Article history:
Received 6 December 2017
Received in revised form
20 March 2018
Accepted 22 March 2018

Keywords:
Nuclear materials
Energy loss
Hydrogen isotopes

ABSTRACT

This work studies the energy loss by different mechanisms in materials of nuclear interest (Al, Ti, Fe) when these are irradiated with an hydrogenic beam. The materials chosen were aluminum, titanium and iron, and the selected beam energy was of the order of 100 keV. The mechanisms considered for energy loss are electron excitation and phonon production, for both of them two quantities are defined: one to compare energy deposition by a single ion beam in different materials, the other to characterize several beams impinging a given material.

Introduction

Ion irradiation in metals is a field of great interest due to technological applications such as ion implantation technology, lithography, aerospace and nuclear technology [1–6]. Moreover, the continuum research in condensed matter and in particular metallic materials supports the development of different industries (e.g. steels, aluminum and titanium) [7,8].

Among the physical quantities involved in the interaction of radiation with matter, the range of the particles in the material and the energy dissipation mechanisms must be specifically taken into account. On the one hand, the range is an average distance that characterizes the particle trajectory inside the material until it loses all its energy. On the other hand, the mechanisms for energy loss depend on the characteristics of the material under irradiation and are a function of the beam energy.

Energetic ions interact with matter by three different mechanisms: (1) Collisions with nuclei, (2) Collisions with electrons and (3) Nuclear reactions at very high beam energies. At high non relativistic energies, the ion-nucleus interactions are classical binary collisions under a Coulomb repulsive potential. Since the ion mass is 1800 times higher than the electron mass, the interaction of ions with electrons does not change its trajectory. In addition, nuclear reactions occur at very high incident energies and involve energy loss by the creation of new atomic species from the target atoms. This last phenomena is out of the scope of the present work given the energy range considered.

Due to the large number of collisions that occurs at high energies, each of the three mechanisms are averaged and

* Corresponding author.
E-mail addresses: mauricio.petaccia@cab.cnea.gov.ar (M.G. Petaccia), gervason@cab.cnea.gov.ar (J.L. Gervasoni).
https://doi.org/10.1016/j.ijhydene.2018.03.152

described separately by the corresponding stopping powers [9] leading thus to a total stopping power given by:

$$S(E) = S_e(E) + S_n(E)[+ S_{reactions}(E)] \quad (1)$$

here $S_e(E)$ is the electronic stopping power and accounts for energy losses involving excitation of the electrons present in the target, $S_n(E)$ is the nuclear stopping power that considers the interactions with nuclei in the material, and $S_{reactions}(E)$ stands for the occurrence of nuclear reactions that will be neglected as mentioned previously.

For $S_e(E)$ the excitation processes taken into account are atomic electron and collective (plasmons) excitations, whereas for $S_n(E)$ there are two mechanisms that are considered: the creation of phonons in the material and the radiation damage process. This work studies the energy loss due to phonon production in Aluminum, Titanium and Iron under irradiation of Hydrogen isotopes with energies of the order of 100 keV. As mentioned before these materials are of great importance in several industries and for technological development.

Simulation methods

In order to study the first instants of irradiation in a material, a simple binary collision approximation (BCA) is used. Such a program generates a continually branching sequence of two-atom collisions in each of which a beam atom collides with an initially stationary target atom. The cascade is initiated by the ejection of a primary knock-on atom (PKA) from an atom site by a ion from the beam. This PKA is the first projectile atom in the simulation. It subsequently collides with the first target atom and, in general, both the projectile and target atom emerge from the collision with enough energy to induce a new collision.

To carry out this study the IM3D code [10] (based on BCA) was chosen. It uses the TRIM-SRIM [11] database which has been extensively used to study different situations [12–15]. In addition, it offers the very useful alternative of parallel computing reducing considerably the CPU time.

IM3D [10] is a massively parallel, open-source, 3D Monte Carlo code for simulating the transport of ions and the production of defects within different materials. IM3D can model the 3D distribution of ions and the material evolution associated with the ions energy loss, such as displacement, sputtering, damage, ionization, and phonon production.

The code computes random trajectories of ions to give statistically meaningful data. Each trajectory corresponds to a particle (ion or knocked target atom) with a specified starting position, a given direction, and an incident or primary energy. The particle is tracked as a random sequence of straight free-flight-paths, ending in a binary nuclear collision event where the particle changes its direction of movement and/or loses energy as a result of nuclear and electronic interactions.

The projectile proliferation in a cascade does not continue indefinitely. At each collision, the projectile kinetic energy is subdivided into three contributions: (1) target atom kinetic energy; (2) reduced projectile atom kinetic energy; and (3) electronic excitation energy. As a consequence of this progressive energy subdivision, either one or both collision partners will eventually fail to induce a new collision and, as a consequence, the cascade eventually dies out.

Since the target atoms are in fixed positions at the beginning of each cascade the temperature of the bombarded material is $T = 0$K.W hen the beam particles impinge the target, the temperature will locally rise but this heat will be conducted or radiated out to the surroundings, and the local temperature falls back to 0 K with no more atom movement.

Results and discussion

This section discusses the results of simulations regarding irradiation of Al, Ti and Fe with H and its isotopes. The energy for the proton, deuterium and tritium beams were chosen to be of the order of 100 keV. The energy loss depth distributions for electron excitation as well as phonon production are discussed for selected cases. In addition, data treatment is performed in order to compare materials and characterize different beams.

Fig. 1 shows a comparison of the energy loss depth distributions in aluminum for a 160 keV beam of protons. It is observed that the energy loss due to electron excitations is two orders of magnitude larger than the corresponding due to phonon excitations. In addition, the depth distribution associated with electron excitations is practically almost constant along the entire ion trajectory. On the other hand the depth distribution for phonon excitations reaches a maximum at large depths. This means that the ion loses energy mainly due to interactions with electrons and afterwards it interacts with nuclei producing lattice vibrations. This is verified by comparing this result with Fig. 2 where the range for different ions are exhibited: the position of the maximum of the energy loss to phonon excitation is similar to the range for this energy (160 keV).

However, this behavior for the energy loss depth distributions is understood by looking at Fig. 3 that exhibits the different components of the stopping power for protons in aluminum in the energy range of interest. It is observed that

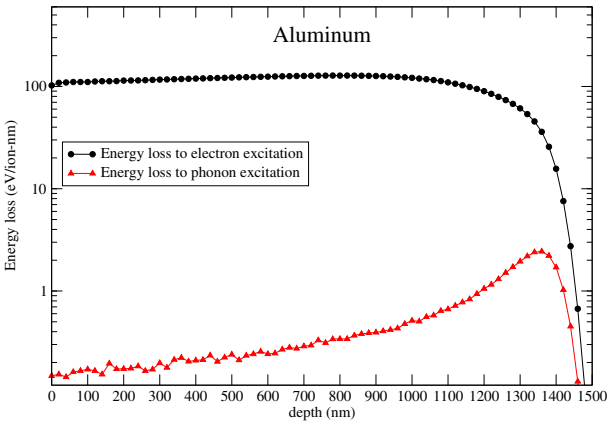

Fig. 1 – Protons energy loss depth distributions to electron (black circles) and phonon (red triangles) excitations in aluminum. Beam energy = 160 keV. (For interpretation of the references to color/colour in this figure legend, the reader is referred to the Web version of this article.)

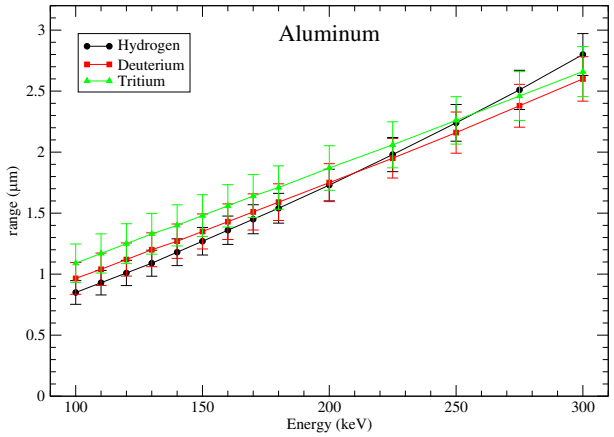

Fig. 2 – Ranges for the three different hydrogen isotopes in aluminum as a function of energy.

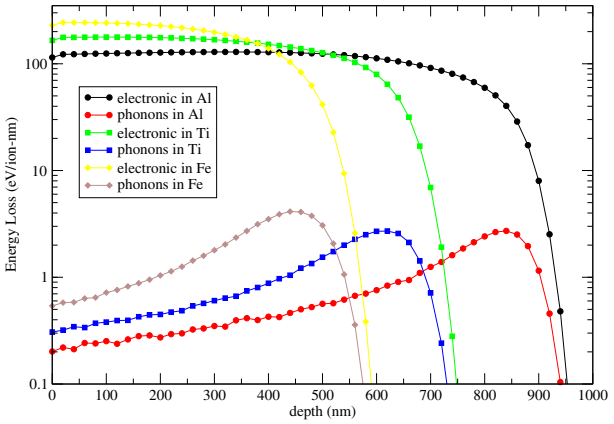

Fig. 4 – Protons energy loss depth distributions to electron and phonon excitations in aluminum, titanium and iron. Beam energy = 100 keV.

the electronic stopping power is two orders of magnitude larger than the nuclear stopping power for all energies, as expected.

All the cases under study are compared for a 100 keV proton beam in Fig. 4. The energy loss depth distribution due to electron excitation falls to zero at smaller depths as the atomic number of the target increases. In addition, more energy is lost for high atomic number materials. These differences between the electron excitation energy loss depth distributions arise because, for high Z materials, there are more electrons available in the target to stop the incident proton, therefore the energy loss under this mechanism is higher. On the other hand, when considering energy loss due to phonon production, the atomic density of the target is a fundamental parameter: more target atoms are available when density increases.

It is worth noticing that the fraction energy devoted to electron as well as phonon excitation is independent of the material and the beam energy being of 5% for electron and about 0.05% for phonon excitations. The same results are obtained when applying a data integration procedure for different particle beams (i.e. deuterium and tritium).

Fig. 5 shows the results obtained in the case of phonon production when a titanium target is irradiated with a deuterium beam. It is observed that the peak moves to deeper regions of the target and decreases when the beam energy increases. Although the first behavior is expected, the second is not. In order to understand the decreasing maximum, it must be emphasized that the representative quantity is the total energy loss, given by the area under the distributions. Data integration shows that this area increases with increasing beam energies, so more phonons are produced per incident ion under this condition.

Fig. 6 illustrates the behavior of the energy loss depth distribution for phonon production when the different 300 keV hydrogen isotopes pass through iron. The maximum of the distribution is displaced when the ion mass increases. It is observed that protons losses less energy to phonon excitation than the other two cases, this is explained considering that the maximum energy transfer in a classical elastic collision, for beam particles lighter than target nuclei, is given by:

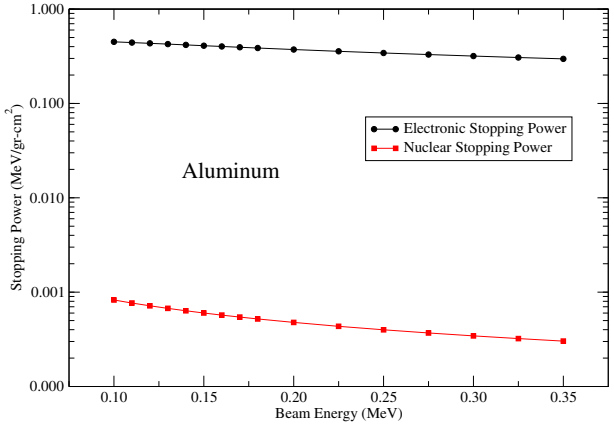

Fig. 3 – Electronic (black circles) and nuclear (red squares) Stopping Powers for protons in aluminum. (For interpretation of the references to color/colour in this figure legend, the reader is referred to the Web version of this article.)

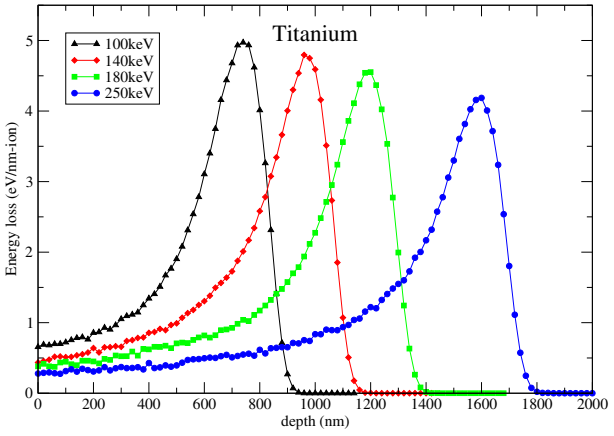

Fig. 5 – Energy loss to phonon excitation by a beam of deuterium into Titanium at different energies.

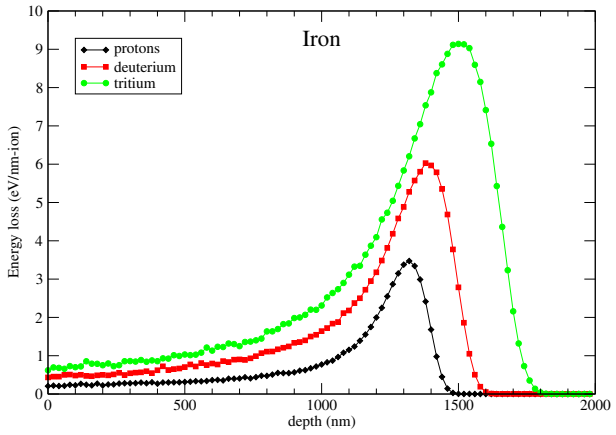

Fig. 6 – Energy loss to phonon excitation by beams of the different hydrogen isotopes at 300 keV into Fe.

$$T_{max} = 4\frac{m_p}{m_t}E\left(1+\frac{E}{2m_pc^2}\right), \quad (2)$$

where m_p is the projectile mass, m_t the target atom mass, E stands for the beam energy and c is the speed of light [16]. It is observed that this quantity increases with m_p when all the remaining parameters are fixed as is the case exhibited in Fig. 6.

A comparison of the total energy devoted to produce electron and phonon excitation by each isotope in each material is performed: all the depth distributions $\phi_{ion,mat}$ are integrated with respect to z, resulting in energy dependent functions:

$$W_{ion,mat}(E) = \int_0^{z_{max}} \phi_{ion,mat}(E,z)dz, \quad (3)$$

where z is the depth coordinate and E stands for the beam energy. The integration limits are the target surface $(z=0)$ and the maximum depth where energy is deposited $(z=z_{max})$.

These energy functions are then compared for different materials taking the aluminum as the reference i.e. the ratios given by:

$$\alpha^{ion}_{X,Al}(E) = \frac{W_{ion,X}(E)}{W_{ion,Al}(E)} \quad (4)$$

are assessed. In the above formula X stands either for titanium or iron.

The results of the analysis described above are shown in Tables 1 and 2 for the case of phonon production and electron excitation respectively. As can be observed (see Table 1), $\alpha^{ion}_{Ti,Al}(E)\simeq 1$ and remains constant independently of the beam energy and ion mass. This means that energy used to produce phonons in Ti and Al are practically the same when adding up all depth contributions.

On the other hand, when electronic excitation is considered the ratios $\alpha^{ion}_{Fe,Al}(E)\simeq 1$ for all practical purposes in every situation studied along this work.

A similar analysis is performed to compare the three different beams for a fixed target material. The functions defined by:

$$\beta^{ion,proton}_{mat}(E) = \frac{W_{ion,mat}(E)}{W_{proton,mat}(E)} \quad (5)$$

are calculated by considering the proton beam as reference, and the results are shown in Table 3 for the case of energy loss to phonon production by deuterium irradiation. It is observed that the quantity $\beta^{D,p}_{mat}$ does not exhibit large variations with respect to the beam energy or to the material under irradiation.

Table 1 – Relative energy loss to phonon production in titanium as a function of beam energy for different ion beams.

E(keV)	$\alpha^{protons}_{Ti,Al}$	$\alpha^{deuterium}_{Ti,Al}$	$\alpha^{tritium}_{Ti,Al}$
100	0.980	0.965	1.011
120	1.015	0.979	0.991
140	1.017	0.981	0.999
160	1.016	0.999	1.007
180	1.017	0.997	1.014
200	0.993	0.994	1.034
250	1.087	1.040	1.034
300	1.010	1.049	1.033

Table 2 – Relative energy loss to electron excitation in iron as a function of beam energy for different ion beams.

E(keV)	$\alpha^{protons}_{Fe,Al}$	$\alpha^{deuterium}_{Fe,Al}$	$\alpha^{tritium}_{Fe,Al}$
100	1.011	0.994	0.995
120	1.017	0.995	0.998
140	1.020	0.996	1.007
160	1.023	0.999	1.006
180	1.024	1.001	1.011
200	1.024	1.003	1.018
250	1.059	1.015	1.028
300	1.048	1.020	1.037

Table 3 – Comparison of the relative energy loss to phonon production by deuterium irradiation for different materials as a function of the beam energy.

E(keV)	$\beta^{D,p}_{Al}$	$\beta^{D,p}_{Ti}$	$\beta^{D,p}_{Fe}$
100	2.465	2.429	2.510
120	2.510	2.422	2.489
140	2.472	2.384	2.437
160	2.413	2.371	2.398
180	2.386	2.340	2.387
200	2.281	2.282	2.374
250	2.398	2.295	2.303
300	2.205	2.292	2.276

Conclusions

The energy loss for hydrogen, deuterium and tritium was studied in three different materials of nuclear interest at several beam energies using the IM3D code. A difference of two orders of magnitude is found between the electron and phonon excitation energy loss depth distributions for all the cases under study. The ranges of all hydrogen isotopes are calculated and a coincidence with the phonon production depth distribution is found. These different depth distributions are compared by assessing the amount of energy devoted to each process (electron excitation and phonon production).

For a fixed ion beam the quantity α is defined to compare energy deposition in different materials. In the case of phonon production, similarities in this parameter are found between Ti and Al at all beam energies. On the other hand, when considering electron excitation, comparing Fe with Al show similar results.

In addition, for each material, all the ion beams are characterized by comparing the total energy deposition of a given isotope with respect to an proton beam (β). It is observed that variations in these quantity are small when different materials are used for the characterization and also when the beam energy is changed.

The study of phenomena such as ion implantation, vacancies production and defect creation as well as other radiation damage effects on these materials is under way.

Acknowledgements

This work was financially supported by Consejo Nacional de Investigaciones Científicas y Técnicas (CONICET) and by the Controlled Nuclear Fusion Program of the Comisión Nacional de Energía Atómica (CNEA) form Argentina.

REFERENCES

[1] Thornell G, Spohr R, van Veldhuizen EJ, Hjort K. Micromachining by ion track lithography. Sensor Actuator Phys 1999;73(1):176–83.
[2] Tokunaga K, Baldwin M, Doerner R, Noda N, Kubota Y, Yoshida N, et al. Blister formation and deuterium retention on tungsten exposed to low energy and high flux deuterium plasma. J Nucl Mater 2005;337:887–91.
[3] Sang C, Sun J, Bonnin X, Guo H, Wang D. Simulation of hydrogen isotope retention in the gap of tungsten divertor tiles. J Nucl Mater 2013;438:S1129–33.
[4] Bo/ttiger J, Picraux S, Rud N, Laursen T. Trapping of hydrogen isotopes in molybdenum and niobium predamaged by ion implantation. J Appl Phys 1977;48(3):920–6.
[5] Alimov VK, Roth J. Hydrogen isotope retention in plasma-facing materials: review of recent experimental results. Phys Scripta 2007;T128:6.
[6] Roth J, Schmid K. Hydrogen in tungsten as plasma-facing material. Phys Scripta 2011;T145:014031.
[7] Renger T, Sznajder M, Geppert U. Experimental studies of low energy proton irradiation of thin vacuum deposited aluminum layers. In: 13th European conference on spacecraft structures, materials and environmental testing; 2014.
[8] Zinkle SJ, Busby JT. Structural materials for fission & fusion energy. Mater Today 2009;12(11):12–9.
[9] Was GS. Fundamentals of radiation materials science: metals and alloys. Springer; 2016.
[10] Li YG, Yang Y, Short MP, Ding ZJ, Zeng Z, Li J. IM3D: a parallel Monte Carlo code for efficient simulations of primary radiation displacements and damage in 3D geometry. Sci Rep 2015;5:18130.
[11] Ziegler JF, Ziegler MD, Biersack JP. SRIM—The stopping and range of ions in matter. Nucl Instrum Methods Phys Res Sect B Beam Interact Mater Atoms 2010;268(11):1818–23.
[12] Robinson MT, Torrens IM. Computer simulation of atomic-displacement cascades in solids in the binary-collision approximation. Phys Rev B 1974;9(12):5008.
[13] Stoller RE, Toloczko MB, Was GS, Certain AG, Dwaraknath S, Garner FA. On the use of SRIM for computing radiation damage exposure. Nucl Instrum Methods Phys Res Sect B Beam Interact Mater Atoms 2013;310:75–80.
[14] Bentini G, Bianconi M, Correra L, Chiarini M, Mazzoldi P, Sada C, et al. Damage effects produced in the near-surface region of x-cut LiNbO 3 by low dose, high energy implantation of nitrogen, oxygen, and fluorine ions. J Appl Phys 2004;96(1):242–7.
[15] Bettiol A, Rao SV, Sum T, Van Kan J, Watt F. Fabrication of optical waveguides using proton beam writing. J Cryst Growth 2006;288(1):209–12.
[16] Carron NJ. An introduction to the passage of energetic particles through matter. CRC Press; 2006.